

Simulation of surface plasmon resonance (SPR) layers of gold with silicon nitride as a Bi-layer biosensor

F. J. Kadhum^a, S. H. Kafi^a, A. J. Karam^{b,*}, A. A. Al-Zuky^a, M. F. H. Al-Kadhemy^a, A. H. Al-Saleh^c

^a*Mustansiriyah University - College of Science- Physics Dept.*

^b*Universities of Garmian, College of Computer and Information Technology, Department of Information Technology, Kurdistan Region - Iraq*

^c*Mustansiriyah University - College of Science- Dept. of computer, Baghdad, Iraq*

Surface Plasmon Resonance (SPR) has gotten a lot of attention in biomedical sensing. Many applications in medical diagnostics and single molecule detection have sparked interest in bio-sensing techniques. Surface Plasmon resonance (SPR) is an important phenomenon used for building sensors especially in the Biological fields. Simulation analysis (in Mat lab) has been made for SPR for gold (Au) layer with thickness (40 nm) and layer of silicon nitride (Si₃N₄) with different thickness (10- 70 nm) step 10, deposited on glass prism type N-LASF9_ glass with the sensitive layer was water at refractive index ($\Delta n = 0, 0.01, 0.05$ and 0.1). The analysis was taken for different wavelengths from Ultra-Violet wavelength 100 nm to Near Infra- Red wavelength 1000 nm. The properties of the surface Plasmon resonance angle (θ_{SPR}) have been calculated from plotted reflectance against incident angle θ_{incid} shows sharper resonance dip, narrower full width half maximum (FWHM), SPR dip length (L_d) increased so that improve in properties SPR and system. The SPR sensitivity (S) was calculated and recorded higher sensitivity about 134.

(Received January 7, 2022; Accepted May 20, 2022)

Keywords: Surface plasmon resonance (SPR), Gold, Silicon nitride, Theoretical model, Sensitivity, Biosensor

1. Introduction

Surface Plasmon Resonance (SPR) is an optical technique widely used to observe the physical or chemical changes occurring at a metal-dielectric interface. Due to its highly sensitive behavior and capability of sensing for label-free sensing, this phenomenon has been featured as a potent optical detection technique [1,2]. SPR sensors have made significant developments in bio-sensing and chemical sensing applications : which took many application areas, including biological and medical diagnostics, and the sensing of chemical and biological pollution in fluids [3,4]. The process of building an optical system for SPR sensor is extremely complicated and extravagant. So, many scientists and researchers have gone to use simulation methods for the purpose of solving this problem and reducing the cost and time when studying important parameters by building SPR sensing systems before their subsequent practical application [5]. SPR sensor technology has become a pioneering and promising technology due to its various advantages. To detect changes in the refractive index of the detecting medium, the sensor must have a quick reaction, be compact in size, and have high sensitivity [6]. Parameters affecting the response and performance of SPR sensors are: thickness of the metal and dielectric layers and their refractive indexes, the number of layers and the differences in layer composition which may vary depending on the design required by the application. It is sometimes necessary to improve the metal and dielectric layers in order to improve the sensor performance [7].

There are several researchers who have studied the SPR sensor system and have worked to design and simulate SPR systems to act as sensors to detect any change in the optical properties of the media under study. Among the most important of these studies: Vladimir Lioubimov, et al.(2004) [8], When an oscillating voltage was supplied to a gold sheet on which surface Plasmon was stimulated, the SPR angle changed. As an adjacent medium, the SPR angle moved for various

*Corresponding authors: ali.jabbar@garmian.edu.krd

<https://doi.org/10.15251/DJNB.2022.172.623>

aqueous solutions. The model was created to account for charge redistribution to the double layer near the liquid-metallic interface as well as gold film deterioration. Mathcad software was used by Fontana E. in (2006) [9], to determine the optimum thickness of the maximum SPR sensitivity based on the incident light wavelength. Wu L. et al. 2010 [10], They confirmed that the SPR biosensor made of graphene deposition on gold was more sensitive than the typical SPR thin gold biosensor. The higher absorption of biomolecules onto graphene is connected to the greater sensitivity. Y. Deng and G. Liu. In (2010) [11], they simulated and designed a prism-based SPR sensor adopting the Kretschmann configuration. A prism-multilayer structure with increased SPR detection has the advantages of higher contrast and sensitivity. A BK7 prism was coated with an Au thin coating (1.8 nm). A photodetector monitored a probe beam of a semiconductor 650nm laser incident on a prism-metallic film interface, as well as the reflected beam, as a function of incidence angle. M.S. Islam et al. (2011) [12] A layer surface Plasmon resonance (LSPR) biosensor with a layer of graphene sheet on top of the gold layer improved its sensitivity and absorption efficiency. With a shorter working wavelength and more graphene layers, the LSPR graphene biosensor offers higher sensitivity. H. K. Rouf, and T. Haque (2018) [13]: They designed a bimetallic surface Plasmon resonance (SPR) sensor (a pair of silver (Ag) - gold (Au)). In addition to the use of a thin layer of indium phosphide (InP) and an air gap layer. They studied different reflectivity curves and performance parameters. The ability of the proposed biosensor to detect 1/1000 of the RIU variation of the sensing medium (caused by changing the analytic concentration) was demonstrated. A. K. Sharma and A. K. Pandey (2019) [14] In the optical communication band, they suggested a self-referencing SPR sensor with a titanium oxide (TiO_2) grating on a thin gold (Au) layer over dielectric substrates. To simulate the sensor and analyze performance parameters, they employed the rigorous coupling wave analysis (RCWA) approach. For the ideal settings of the grating variables, they got a mean spectral sensitivity (S) and an SPR curve width of 693.88 nm/RIU and 26.03 nm, respectively. For a wide range of analytical refractive indices, the use of TiO_2 as a grating on an Au film over a SiO_2 substrate can give more sensitivity than grating-based plasmonic sensors. H. Akafzade, et al (2020) [15] they used single-layer and multi-layer metal Ag / Si_3N_4 / Au sensors to monitor the changes in the refractive index of glucose/water solutions. According to the findings, the sensor can resolve the refractive index of glucose down to a concentration of 1 % – 4 %. They discovered that this sensor can detect a 0.0001 change in refractive index and is suited for biological and medicinal applications. H. Akafzade et al (2021) [16] They demonstrated a novel form of SPR sensor made from a multilayer Ag/ Si_3N_4 /Au nanostructure. This sensor performed well in determining the relative concentration of glucose in glucose/water mixtures. According to computer simulations, the electric field on the surface of this multi-layer sensor is up to 50% greater than the field on the surface of the gold film sensor.

In this study, a simulation program was created by adopting Fresnel equations for the reflectivity of electromagnetic waves in the range (100 nm to 1000 nm) and by using the transfer matrix of a system consisting of a semicircular prism on which two layers are deposited: the first is gold (Au) with a thickness of 40 nm and the second is nitride Silicon (Si_3N_4) is a thin film with variable thickness starting from 10 nm to 70 nm and the sensitive medium is water. The complex refractive indices of the materials approved in the study (semicircular prism glass N-LASF9, gold, and silicon nitride (Si_3N_4)) were obtained from the database available on the website (refractiveindex.info) [17].

2. Methodology

Transfer matrix method is used in optics to analyze the propagation of electromagnetic waves through a stratified medium. It allows calculations of the reflectance, transmission, and emission spectra in facilitating additional evaluations the guided modes and band diagrams for multilayered structures. The transfer matrix method is based on Maxwell's equations, and relies on simple continuity conditions for an electric field across boundaries from one medium to another [18]. A stack of layers can be represented as a system array, which is the product of special layer arrays. The final step of the method contains converting the system matrix back into reflection and transmission coefficients. The propagation matrix equation obtained by applying the boundary

condition for the propagation of electromagnetic (EM) waves at the interface between N layers in the SPR sensor stack apart from the prism, tangential components of electric and magnetic fields firstly (E_a and B_a) and finally (E_N and B_N) boundaries may be expressed as[19]:

$$\begin{bmatrix} E_a \\ B_a \end{bmatrix} = \left[\prod_{i=1}^N M_i \right] \begin{bmatrix} E_N \\ B_N \end{bmatrix} = \begin{bmatrix} m_{11} & m_{12} \\ m_{21} & m_{22} \end{bmatrix} \begin{bmatrix} E_N \\ B_N \end{bmatrix} \quad (1)$$

M_i : is the i^{th} characteristic matrix of this structure, where for the i^{th} layer stacked between the prism and the sensing layer, which is given by [20]:

$$M_i = \begin{bmatrix} \cos\delta_i & \frac{i\sin\delta_i}{\gamma_i} \\ i\gamma_i\sin\delta_i & \cos\delta_i \end{bmatrix} \quad (2)$$

Where γ_i : is the propagation constant for i^{th} layer and δ_i : The optical phase addition is caused by a single field traversal across the i^{th} layer, which is given by [17]:

$$\delta_i = \left(\frac{2\pi}{\lambda} \right) n_i d_i \cos\theta_i \quad (3)$$

Where λ : is the vacuum light wavelength, n_i : is the refractive index, and d_i : is the thickness, and θ_i : the incidence angle for i^{th} layer.

γ_i For p-polarization EM wave given by [21]:

$$\gamma_i = \frac{n_i \sqrt{\epsilon_0 \mu_0}}{\cos\theta_i} \quad (4)$$

Where ϵ_0 : the permittivity and μ_0 : permeability in vacuum.

The characteristic matrix M_i describes the behavior of all intervening layers. In Eq.(1) where the electric and magnetic fields in the i^{th} layer were coupled to the M_i interference matrix of that layer at both interfaces. The total interference matrix of the whole multilayer structure was calculated using the transverse components of the electrical and magnetic fields, which are continuous at each contact that is free of net charge and current : $M = \prod_{i=1}^N M_i$, this equation can be obtained the reflection coefficient r and transmission coefficient t through the films from these matrices as[21]:

$$r = \frac{\gamma_N m_{11} + \gamma_0 \gamma_N m_{12} - m_{21} - \gamma_0 m_{22}}{\gamma_N m_{11} + \gamma_0 \gamma_N m_{12} + m_{21} + \gamma_0 m_{22}} \quad (5)$$

$$t = \frac{2\gamma_0 \left(\frac{n_N}{n_0} \right)}{\gamma_N m_{11} + \gamma_0 \gamma_N m_{12} + m_{21} + \gamma_0 m_{22}} \quad (6)$$

From Eq.(5) reflectance can be calculated ($R = |r|^2$) to obtain pattern of redistribution of incident light energy into SPR waves, and thus reflected field power as a function of incident angle can be obtained. Similarity, from eq. (6) transmission can be calculated ($T = |t|^2$). The sensitivity of biosensors is an essential factor to consider while trying to increase their effectiveness. It is determined by the operating wavelength and material properties, such as the dielectric layer's refractive index, the refractive index of the prism, the metal film, and the film thickness. They're chosen to optimize the resonance condition, which is described as [22]:

$$k_{spr} = \frac{\omega}{c} \sqrt{\frac{\epsilon_1 \epsilon_2}{\epsilon_1 - \epsilon_2}} \quad (7)$$

Where c denotes the speed of light in a vacuum, ω denotes the light frequency, and ϵ_1 , ϵ_2 are the dielectric constants of the metal and the medium in contact with it, respectively. The dielectric constant of metal $\epsilon = \epsilon_r - i \epsilon_i$ [22], is linked to optical constants by the expressions $\epsilon_r = n^2 - k^2$ and $\epsilon_i = 2nk$, where n and k are the medium's index of refraction and extinction coefficient, respectively.

The frequency-dependent refractive indices of the metal, the dielectric thickness and structural quality of the metal film, and the sensor's long-term stability are the primary determinants of the sensor's performance characteristics (quality), especially when the sensor is used in contact with reactive analytic materials. High sensitivity is attained by achieving a large shift of resonance angle (in phase interrogation) or resonance wavelength (in wavelength interrogation) with a small change in (refractive index, thickness and concentration) [23]. SPR is a very good sensor, due to it is very sensitive to any chemical change in the metal surface, this is due to the change in k -vector of the Plasmon when the composition of the medium changes, so the angle of incident light at which the resonance occurs changes with large amount due to the fact that the field at the interface between the metal and the upper dielectric is greatly enhanced, and this can be measured very carefully. SPR is dependencies on: metallic film properties, incident light wavelength, and refractive indices of the media on both sides of the metallic film sensitive to temperature [24].

The schematic diagram of the proposed SPR sensor is shown in Fig.1. Gold is used in most plasmonic detectors because it has various advantages, including being chemically inert, long-term stable, and easy to shape [25]. As a result, it has more optical damping and a broader resonance wavelength dip, which leads to false-positive analytic detections. [26]. Gold has free electrons that are excited at optical wavelengths longer than about 500 nanometers, when electron excitation occurs the light will be absorbed. The dielectric layer of silicon nitride (Si_3N_4) provides many exceptional properties; it is optically transparent in the range from UV to IR (250-900) nm, it has a relatively large refractive index, Thermal stability, hardness, chemical inertness, and strong insulating qualities are all important considerations. The Si_3N_4 dielectric's widespread application in the extremely large-scale integrated electronic production and processing sector justifies it.[23].

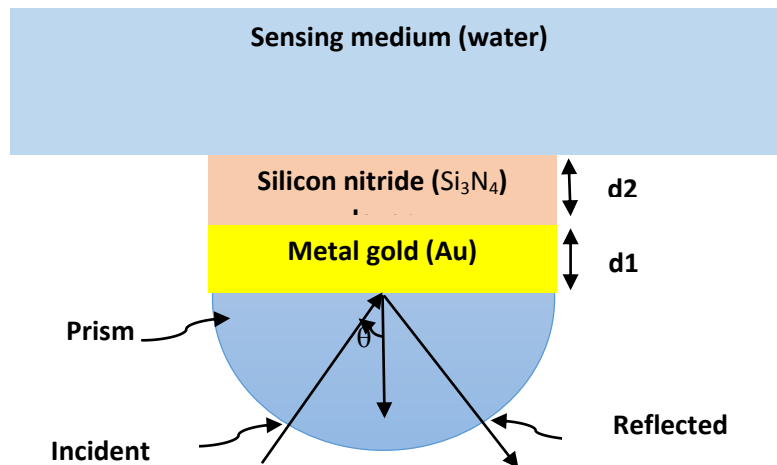


Fig. 1. Schematic diagram of the proposed SPR sensor (glass prism half sphere).

In the simulation steps, an electromagnetic wave with wavelengths ranging from 100nm to 1000nms was adopted to find spectrum regions where the SPR phenomenon occurs. In this study a Kretschmann configuration with an N-LASF9 glass half sphere prism was used. A gold (Au) sheet with a continuous thickness of 40 nm was deposited on the prism, and then another layer of silicon nitride (Si_3N_4) was deposited with different thicknesses, with water used as a medium for biological or chemical sensitivity.

The SPR dip must be deep enough, sharp, and of high contrast for the sensor to be effective and good. While, a very wide SPR dip indicates the possibility of a wider range of incident SPR angle, and thus would lead to worse sensitivity for the sensor. Now summarize the parameters to be changed during the simulation:

- Electromagnetic waves: of wavelengths ranged (100nm to 1000nm) step changes 100nm from Ultra-Violet wavelength to Near Infra- Red wavelength.
- Sub phase: water with changing in refractive index by: ($\Delta n = 0, 0.01, 0.05, \text{ and } 0.1$).
- Gold layer thickness: 40nm.
- Dielectric layer thickness (Si_3N_4): (10-70) nm step changes 10nm.

An important note is that as the incident wavelengths change, so the refractive indexes of system materials (prism N-LASF9_ glass, gold, and dielectric (Si_3N_4) and water) will changed. Therefore, in this study, the values of the tables of refractive indexes available on the website (refractive index. Info [17]) were used. The refractive index of the water will also change with the wavelength, but the difference is so small that it can be neglected.) [27].

The simulation program performed by developing Masahiro Yamamoto's algorithms: "Surface Plasmon Resonance (SPR) Theory" [28].

3. Results and discussions

The optimum film thickness of a single metal based SPR sensor has to be such that the resonance curve produced by a sensor structure under consideration not only shows the maximum possible loss in reflectivity but also produces the narrowest possible FWHM of the reflectivity curve. From Figs(2 and 3) show SPR curves for Au 40nm thickness layer, and Si_3N_4 layer of thickness varying from (10 – 70) nm steps 10. The surface Plasmon resonance angle (θ_{SPR}) is the angle of incidence at which the least reflection occurs and corresponds to the highest energy loss owing to surface Plasmon excitation. May be show the changes in the SPR characteristics are:

1. The reflectivity will be greatly reduced at the surface Plasmon resonance angle θ_{SPR} .
2. With a little rise in the refractive index of the sensitive medium, the surface resonance angle of the Plasmon (SPR) is pushed slightly towards higher values.
3. When the wavelength is increased to (1000) nm and the thickness of the Si_3N_4 layer is increased with the rise of the refractive index of the sensitivity medium, the resonance curves sharpen and the FWHM narrows.

Figure (2) shows the relationship between reflectivity and the angle of incidence, when the thickness increases from (10-70) nm. Where there are no SPR is observed at wavelength (100-500) nm for each Si_3N_4 layer thickness. Then it begins to appear at 600 nm for all thicknesses. That is, SPR would appear at wavelengths greater than 600 nm and best SPR would appear at wavelengths of 1000 nm. It was also observed that as the thickness of the dielectric layer increased; the resonance angle would be increased with the increase in the SPR dip width. An important observation is that the SPR dip width will decreased sharply for 1000 nm wavelength with different thicknesses (d). Additionally, it's completely disappeared of SPR at 800 nm wavelengths, and then reappears clearly and strong at wavelengths (900-1000) nm better for previous wavelengths of all Si_3N_4 layer thicknesses. The resonance angle is shifted to the right with an increase in Δn for all thicknesses.

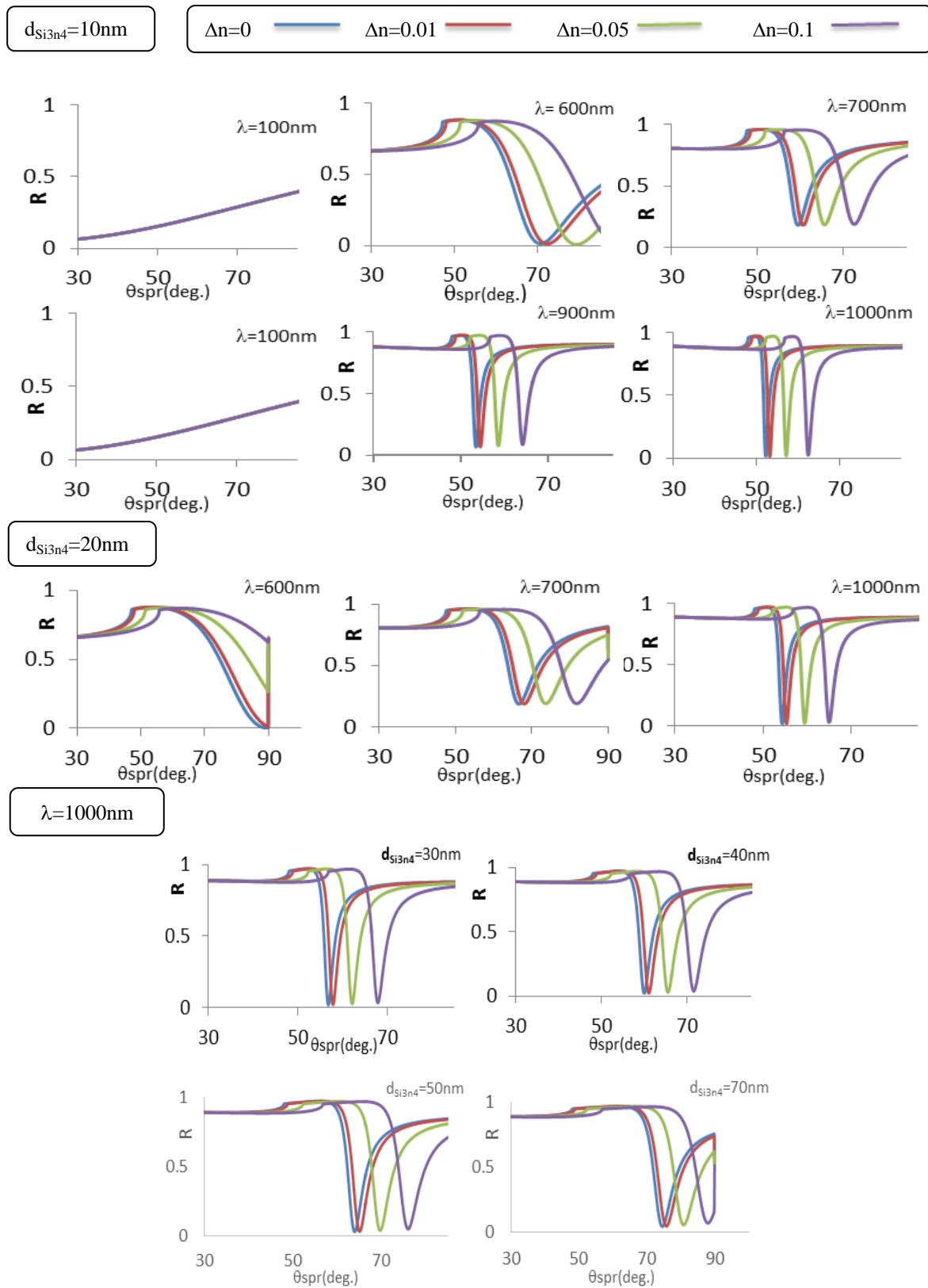


Fig. 2. The relation between reflectance with incident angle for different thickness Si_3N_4 layer and different wavelength.

Figure (3) shows the relationship between resonance angles, θ_{spr} with the thickness of the dielectric layer. The best results at 1000 nm wavelength showed that θ_{spr} increases with increasing

thickness from (10-70) nm, with increasing variation in the sensing medium's refractive index, (outer medium) ($\Delta n=0, 0.01, 0.05, 0.1$).

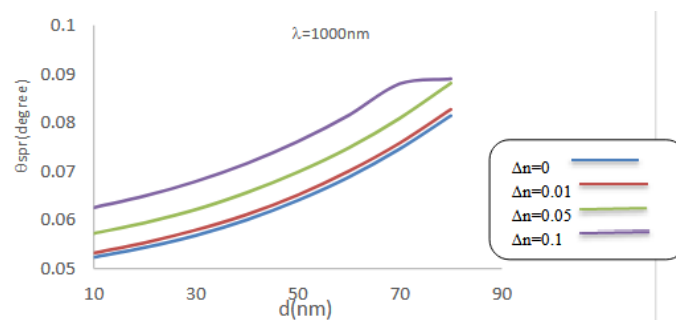


Fig. 3. The relation between the resonant angles SPR with the layer dielectric thicknesses.

Figure (4) illustrated the Full Width Half Maximum (FWHM) and SPR dip length (L_d) with the changing in outer medium refractive index. Noted that the FWHM decreased with increasing Δn at the thickness $d=10\text{nm}$ and $\lambda=600\text{nm}$; FWHM and L_d decreased with increasing refractive index of layer sensing i.e. Increased Δn , well at $\lambda=700\text{nm}$ FWHM slightly increased, L_d is stable with increasing Δn , but at $\lambda=1000\text{nm}$ FWHM stable and L_d almost stable with increasing Δn . Then at $d=20\text{nm}$ and $\lambda=700\text{nm}$ the FWHM decreased, L_d stable with increasing Δn , while at $\lambda=1000\text{nm}$ FWHM starting to increase with increasing Δn and L_d decreased with increasing Δn . So that for other thicknesses from (30-70) nm the best FWHM and L_d shown at 1000nm, notice FWHM at thicknesses $d=(30, 40, 50, \text{ and } 70)\text{ nm}$ increased and L_d almost stable with increased in Δn . This means that the FWHM decreased, L_d increased whenever increased the wavelength and improve in SPR properties then improve in the SPR sensing system. The L_d was higher than 0.8 for all SPR dips for the wavelengths (600, 700, and 1000) nm, and the best values for the L_d were for the SPR dip length at the wavelength of 1000 nm. As the L_d value ranges between (0.9-1) degrees for all Δn . As for the FWHM values when using the thickness at $d=10\text{nm}$ for SPR dip when using the 600 nm wavelength within (22.7-10.7) degrees with a change of, the FWHM values improved and the SPR dip became more narrow when using the 700nm wavelength, where its value became between (6.2 -8.8) degrees with different Δn . Then the FWHM began to decrease further, meaning that the SPR dip became narrower when using the wavelength 1000nm and its FWHM value became between (1.5-2.0) degrees with different Δn . The SPR dip widened when using the thickness $d=20\text{nm}$, where the FWHM values become (26.7-13.1) degrees for the wavelength 700nm with different Δn . At the same thickness, the FWHM of SPR dip at wavelength 1000 nm is stable and dip very narrow and does not change with Δn its values (1.5 degrees). While for the thickness $d=70\text{nm}$ for the same wavelength 1000nm, the value of the SPR dip width ranges between (7.9-4.7) degrees with the change of Δn . Therefore, here the proposed system can be adopted as an effective system to work as a biological sensor within the infrared spectrum region at a wavelength of 1000nm.

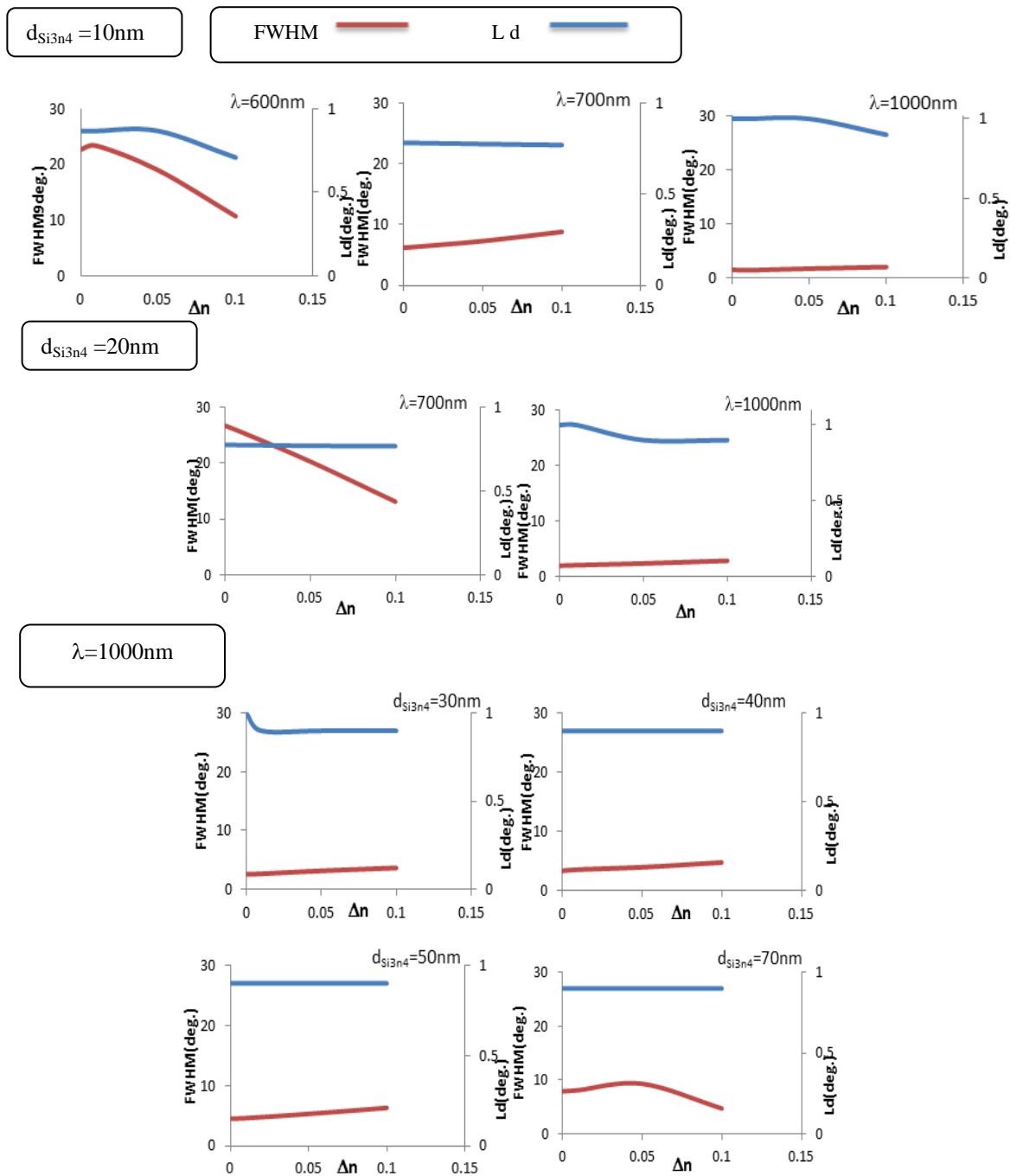


Fig. 4. Full Width Half Maximum (FWHM) and length dip L_d with the change refractive index of layer thin films for different thickness Si_3N_4 and wavelength.

The relationship between sensitivity considering the change of thicknesses of Si_3N_4 layer and the change of sensing medium refractive index $\Delta n = 0.05$ was shown in fig.(5) it will be noticed at $\lambda=700nm$ increased in sensitivity with increasing thickness from(10-30)nm in visible region. While at $\lambda=900nm$ increased in sensitivity with increasing thickness from (10-50) nm in IR-region and at $\lambda=1000nm$ increased in sensitivity with increasing thickness from (10-70) nm in IR-region, this means that the best result for sensitivity obtained in 1000nm IR-region. The best sensitivity values (S) were when using the wavelength $\lambda=1000nm$, where its values ranged between ($S = 98-134$) as for thicknesses from $d = (10-70)$ nm and $\Delta n=0.05$.

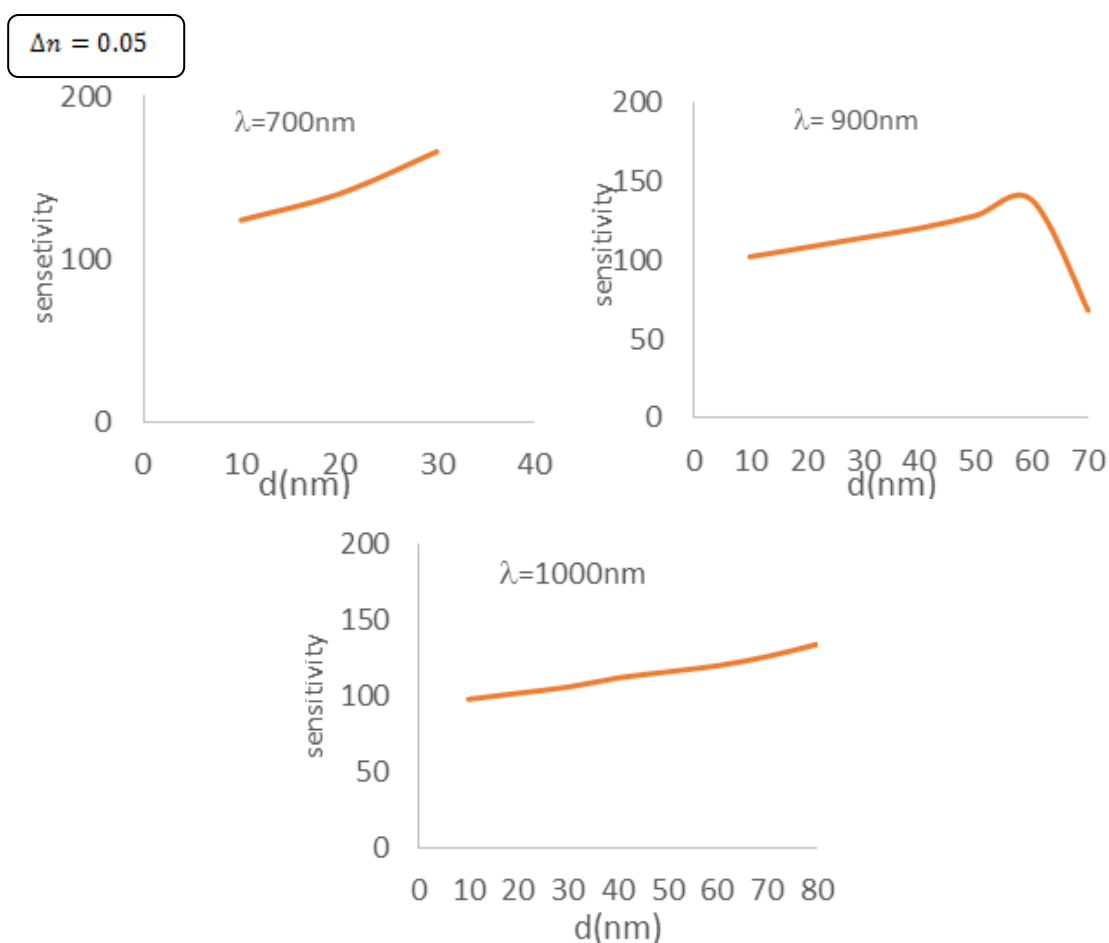


Fig. 5. Illustrated sensitivity with respect to thicknesses of Si_3N_4 layer at different wavelength with refractive index $\Delta n = 0.05$.

4. Conclusions

In this article, a simulation tool for calculating the SPR effect in a multilayer structure is provided. Simulation-SPR is a program that analyzes the reflectance of a prism-based system, the SPR sensitivity (S) and Full Width Half Maximum (FWHM), and the properties of θ_{SPR} calculated from curve reflectance with incident angle θ_{incid} . May show the changes in the SPR, the reflectance suffers loss at resonance, the angle of the surface Plasmon resonance (θ_{SPR}) changes upward. The FWHM narrows as the resonance curves get sharper, and the magnitude of the loss in reflectivity decreases. The results give efficient detection in change of sensitive layer refractive index (0, 0.01, 0.05 and 0.1), and obtained higher sensitivity. In this paper, a simulation algorithm was built to calculate the effect of SPR, taking into account a multi-layered structure consisting of a glass prism type N-LASF9_ glass with a gold layer of 40nm thickness, on which Si_3N_4 layers of different thicknesses from 10nm to 70nm were deposited with water as a sensitization medium. Where notice that in the simulation system SPR phenomenon does not appear in the ultraviolet region and appears weak in the visible region, starting from the wavelength of 600nm and up to 700nm. In the infrared region, the SPR dip completely disappears at the wavelength of 800nm then returns to appear strongly at the wavelengths of 900nm and 1000nm.

The results show that the best stabilization that can be obtained for the sensor action is located in the infrared region. It was the best SPR that could function as a water sensor at the wavelength of 1000nm.

The best values for sensitivity S , length L_d , and FWHM of the SPR dip were obtained from the simulation program of the proposed system at using $\lambda=1000\text{nm}$ in the infrared region when using thicknesses, and $d = 10\text{-}70\text{ nm}$, to detect any change in sensing medium refractive index Δn in range (0.01-0.1). Where the values were $L_d = 0.9$ is stable, SPR is very narrow (i.e small and good FWHM less than 9.3degrees) and the sensitivity is $S = 134$ at $\Delta n=0.05$. Here it is possible to suggest using this proposed system as an effective biosensor to work in the infrared region.

Acknowledgements

The authors would like to thank Department of Physics/ College of Science/ Mustansiriyah University (www.uomustansiriyah.edu.iq) Baghdad-Iraq for its support in the present work.

References

- [1] Momota M. R. and Hasan R., "Hollow-core silver coated photonic crystal fiber plasmonic sensor", *optical materials*, 2018, 76, 287-294; <https://doi.org/10.1016/j.optmat.2017.12.049>
- [2] Berger C.E., Greve J., "Differential SPR immune sensing", *Sensor. Actuator. B Chem.*, 2000, 63 (1), 103-108; [https://doi.org/10.1016/S0925-4005\(00\)00307-5](https://doi.org/10.1016/S0925-4005(00)00307-5)
- [3] Fang Y., "Label-free cell-based assays with optical biosensors in drug discovery", *Assay Drug Dev. Technol.*, 2006, 4 (5), 583-595; <https://doi.org/10.1089/adt.2006.4.583>
4. Homola J., Yee S. S., Gauglitz G., "Surface Plasmon resonance sensors: review.", *Sensors Actuators B Chem*, 1999, 54(1-2), 3-15; [https://doi.org/10.1016/S0925-4005\(98\)00321-9](https://doi.org/10.1016/S0925-4005(98)00321-9)
5. Banerjee J., Bera M., Ray M., "Theoretical differential phase analysis for characterization of aqueous solution using surface Plasmon resonance". *Plasmatic*. 2017, 12(6), 1787-1796; <https://doi.org/10.1007/s11468-016-0446-4>
6. Mokhtar R., Abidin Z., Mat W. M., and Abidin Z., "Multilayers analysis using the phenomenon of surface plasmon resonance", *Journal Fizik Malaysia*, 2007, 28 (3), .
7. Englebienne P., Van Hoonacker A., and Verhas M., "Surface plasmon resonance : principles , methods and applications in biomedical sciences", *J. of Spectroscopy*, 2003, 17, 255-273; <https://doi.org/10.1155/2003/372913>
8. Lioubimov V., Kolomenskii A., Mershin A., Nanopoulos D. V, and Schuessler H. A., "Effect of varying electric potential on surface-plasmon resonance sensing", *Applied Optics*, 2004, 43(17), 3426-3432; <https://doi.org/10.1364/AO.43.003426>
9. Fontana E., "Thickness optimization of metal films for the development of surface-Plasmon-based sensors for nonadsorbing media", *Appl Opt.*, 2006, 45(29), 7632-7642; <https://doi.org/10.1364/AO.45.007632>
10. Wu L., Chu. H. S., Koh. W. S., Li. E. P., "Highly sensitive graphene biosensors based on surface Plasmon resonance", *Opt. Express*, 2010, 18(4), 14395-14400. <https://doi.org/10.1364/OE.18.014395>
11. Deng Y., Guohong L., "Surface Plasmon's resonance detection based on the attenuated total reflection geometry", *procediaengineering* <https://www.sciencedirect.com/science/journal/18777058>, 2010, 7, 432-435; <https://doi.org/10.1016/j.proeng.2010.11.071>
12. Islam M. S., Kouzani A. Z., Dai X. J., Michalski. W. P., Gholamhosseini H., "Comparison of performance parameters for conventional and localized surface Plasmon resonance graphene biosensors", *International Conference of the IEEE EMBS Boston, Massachusetts USA (IEEE, 2011)*, 1851-1854; <https://doi.org/10.1109/IEMBS.2011.6090526>
13. Rouf H. K. and Haque T., "Performance Enhancement of Ag-Au Bimetallic Surface Plasmon Resonance Biosensor using InP", *Progress in Electromagnetics Research*, 2011, 76, 31-42; <https://doi.org/10.2528/PIERM18092503>
14. Anuj K. Sh. and Kumar Pandey A., "Self-referenced plasmatic sensor with TiO₂ grating on thin Au layer: simulated performance analysis in optical communication band", *Journal of the*

- Optical Society of America, 2019, 36(8), F25-F31; <https://doi.org/10.1364/JOSAB.36.000F25>
15. Akafzade H, Hozhabri N, Sharma S.C., "Application of single metal Au and Ag/Si₃N₄/Au plasmonic sensors for glucose refractive index measurements - arXiv preprint arXiv: 2007.00064", 2020 - arxiv.org. Applied Physics (physics. app-ph.) (2020).
16. Akafzadea H. , Hozhabrib N., Sharma S.C., "Highly sensitive plasmonic sensor fabricated with multilayer Ag/Si₃N₄/Au nanostructure for the detection of glucose in glucose/water solutions", Sensors and Actuators A: Physical, 2021, 317(1); <https://doi.org/10.1016/j.sna.2020.112430>
17. RefractiveIndex.INFO website: <https://refractiveindex.info> refractiveindex.info database © 2008-2020 Mikhail Polyanskiy.
18. Born M., Wolf E., "Principles of optics: electromagnetic theory of propagation", interference and diffraction of light. Oxford, Pergamon Press, 1964.
19. Kloos G., Matrix methods for optical layout, SPIE Press, Bellingham, Wash., 2007; <https://doi.org/10.1117/3.737850>
20. Verma R., Gupta B. D., Jha R., "Sensitivity enhancement of a surface Plasmon resonance based biomolecules sensor using graphene and silicon layers", Sens. Actuators, 2011, B160 623-631; <https://doi.org/10.1016/j.snb.2011.08.039>
21. Maharana P. K., Jha R., "Enhancing performance of SPR sensor through electric field intensity enhancement using grapheme", Workshop on Recent Advances in Photonics (WRAP), 17-18 Dec. 2013; <https://doi.org/10.1109/WRAP.2013.6917704>
22. Eduardo Fontana R. H. and Moslehi M., "Characterization of dielectric-coated, metal mirrors using surface Plasmon spectroscopy", Appl. Opt., 1988, 27, 3334-3340; <https://doi.org/10.1364/AO.27.003334>
23. Sharma S., "Surface Plasmon Resonance Sensors : Fundamental Concepts , Selected Techniques" , Materials and Applications, 2018.
24. Fouad S., Sabri N., Jamal Z. A. Z., and Poopalan P., "Surface plasmon resonance sensor sensitivity enhancement using gold-dielectric material", Int. J. Nanoelectronics and Materials, 2017,10, 149-158.
25. Nano films fiber optical taper sea new route towards low-loss hybrid plasmonic modes, Sci. Rep. 5 (2015); <https://doi.org/10.1038/srep17060>
26. Rifat A. A., Ahmed R., Yetisen A.K., "Photonic crystal fiber based plasmonic sensors", Sensor. Actuator. B Chem., 2017, 243, 311-325; <https://doi.org/10.1016/j.snb.2016.11.113>
27. SCHOTT optical glass data sheets 2012-12-04, link: http://refractiveindex.info/download/data/2012/schott_optical_glass_collection_datasheets_dec_2012_us.pdf (2012).
28. Masahiro Yamamoto's online self-study note: Surface Plasmon Resonance (SPR) Theory, link: http://www.chem.konanu.ac.jp/applphys/web_material/spr_tutorial/sprtheory.html ,Review of Polarography, 2002, 48 (3), 209-237